Key Engineering Materials
ISSN: 1662-9795, Vol. 926, pp 1601-1608
doi:10.4028/p-7l74r2

Submitted: 2021-11-30
Revised: 2022-01-24
Accepted: 2022-02-02
Online: 2022-07-22

Drillability of Magnesium-Based Fiber Metal Laminates Obtained via Hot Metal Pressing with Different Metal Surface Treatments

Lucia Lizzul[1,a*], Rachele Bertolini[1,b], Marco Sorgato[1,c], Andrea Ghiotti[1,d] and Stefania Bruschi[1,e]

[1]Department of Industrial Engineering, University of Padova, Via Venezia 1, 35131, Padova, Italy

[a*]lucia.lizzul@unipd.it, [b]rachele.bertolini@unipd.it, [c]marco.sorgato@unipd.it, [d]andrea.ghiotti@unipd.it, [e]stefania.bruschi@unipd.it

*corresponding author

Keywords: Fiber metal laminate, drilling, delamination.

Abstract. The demand for lighter and more performant aerospace and automotive components has resulted in a substantial surge in a recent interest in parts made of Fiber Metal Laminates (FMLs). For such components, drilling operations are crucial for permitting subsequent assembly. However, drillability of fiber metal laminates is critical due to the heterogeneous thermal and mechanical properties of the metal and composite that form the laminate. In this framework, the current research work aims at understanding how drilling operations can be affected by different surface treatments carried out on AZ31B magnesium alloy sheets joined with Glass Fiber Reinforced Polyamide 6 (PA6-GFRP) via hot metal pressing to form the FML. To this end, the Mg/PA6-GFRP/Mg composites were first fabricated using AZ31B surfaces that were previously treated through sandblasting, annealing, and their combination. Dry drilling was then performed using twist and spur drill bits. The feed was also varied, using two levels. The thrust force, hole quality, delamination and fiber pull-out were considered to evaluate the FMLs drillability. Results showed that the magnesium alloy sheet treatment influenced the drillability, and that the drill bit had an effect too. In particular, sheets that were both sandblasted and annealed allowed the highest drillability avoiding delamination. The use of spur drill bits improved the drillability too, reducing the FML inflection under the drill bit load.

Introduction

The need to expand the range of mechanical, chemical and physical properties of materials to meet emerging technological needs has led to the development of composite materials. Increasingly stringent restrictions in the transportation field aimed at reducing CO_2 emissions have pushed research towards materials with high stiffness-to-density and strength-to-density ratios [1]. Research and innovation on metal-based composites in the last decade has particularly affected the subset of Thermoplastic Fiber Metal Laminates (TFMLs) [2,3]. This class of composites combine the properties of light metals with those of Fiber Reinforced Plastics (FRPs) with thermoplastic matrix. The result is a material with optimal impact resistance, superior recyclability and reduced processing time as compared to the conventional FMLs with thermoset plastics [4]. In the last years, the research on magnesium alloys to be utilized as constituent material in FMLs gained attention thanks to their lower density and greater electromagnetic shielding as opposed to the aluminum alloys that are usually utilized [5,6]. Among some fast and cost-effective bonding techniques for TFMLs, there is the Hot Metal Pressing (HMP) process [7,8]. This method consists of the melting of the polymeric matrix, which flows and forms a bond before solidifying when cooled under mild pressure levels. The HMP effectiveness to join AZ31B magnesium alloy sheets with PA6-GFRP was studied in [9]. In this work the AZ31B surfaces were conditioned before joining through mechanical abrasion by sandblasting to increase the surface roughness and through annealing to change the metal surface chemistry. It was proved that the joint strength was enhanced when both mechanical and chemical surface modifications were applied, due to the simultaneous effect of mechanical interlocking and chemical bonding. Although HMP studies are encouraging, this technique is still at a low level of technological readiness, and further studies on the reliability of the joint performance are needed. The

assembly of FMLs for structural purposes usually consists of mechanical screwing that implies the need for drilling operations. However, drillability of FMLs is known to be critical due to the heterogeneous thermal and mechanical properties of the materials that form the laminate [10]. As a consequence, drilling such components may lead to delamination damages and low-quality surfaces that lastly affect the FML in-service performances. To avoid delamination and reduce thrust forces when drilling stacked composites, the geometry of the drill bit can play a major role, but documentation on FMLs is still scarce [11]. In this context, the current research work aims at investigating the drillability of a TFML obtained via HMP composed of two AZ31B magnesium alloy external sheets and a core of PA6-GFRP. The AZ31B sheets were subjected to different surface treatments before HMP, namely sandblasting, annealing, and their combination. The TFMLs thus manufactured underwent dry drilling operations at two different feeds using two different drill bits geometries, namely twist and spur. The thrust force, hole quality, delamination and fiber pull-out were considered to evaluate the actual FML drillability.

Materials and Methods

TFMLs constituent materials. The constituent materials of the investigated TFMLs consisted of 1 mm thick PA6-GFRP sheets (Tepex® dynalite 102-RG600(2) from Lanxess) made up of two layers of woven glass fabric in a 2/2 twill weave fabric, and 0.5 mm thick AZ31B magnesium alloy sheets. The characteristics of the two constituent materials are reported in Table 1.

Table 1. AZ31B and PA6-GFRP sheets characteristics according to the manufacturers' specifications.

	AZ31B	PA6-GFRP	
Composition	3 wt% Al - 1 wt% Zn - 0.35 wt% Mn - Mg balance	Matrix	Reinforcement
		Polyamide 6 $[-NH(CH_2)_5CO-]n$	E-glass roving 47% vol. fraction
Thickness	0.5 mm	2 layers, 0.5 mm each	
Density	1.77 g/cm^3	1.80 g/cm^3	
Elastic modulus	45 GPa	18 GPa	
Ultimate tensile strength	260 MPa	380 MPa	
Yield strength	200 MPa	/	
Strain at fracture	15 %	/	
Crystallite melting temperature	/	220°C	

The microstructures of the two materials were observed after mechanical polishing using a Leica™ DMRE Optical Microscope (OM) equipped with a high definition digital camera. The AZ31B specimens were etched using a picric acid-based solution for 10 s and their grain size measured with the ImageJ™ software. The Vickers microhardness was measured with thirty random indentations across the mounted cross-sections by using the Durimet™ tester by a Leitz with a load of 15 gf according to the ASTM E92-17 standard [12]. The AZ31B magnesium alloy was characterized by a homogeneous and fully recrystallized microstructure, with an average grain size of 9.7 ± 3.2 μm and a microhardness of 40.3 ± 3.1 $HV_{0.015}$. The PA6-GFRP showed the two layers of woven glass fabric with fiber diameter of 16 ± 2 μm.

TFMLs fabrication and typology. Before joining via HMP, the mating surfaces of the AZ31B sheets were treated according to the experimental plan reported in Table 2. The TFML structure and geometry, together with the joining process via HMP, are showed schematically in Fig. 1. The PA6-GFRP sheet is interposed between two AZ31B sheets and then heated close to the crystallite melting

temperature of the thermoplastic matrix under the dies pressure of 1 MPa for bonding to take place. The result is a sound TFML with dimensions 70 mm × 30 mm × 2 mm. The adhesion mechanisms of the PA6 matrix of the GFRP to the AZ31B sheets at varying metal surface treatment are reported in detail in [9], and are here summarized and represented in Fig. 2. The sandblasting treatment leads to a rough metal surface (areal surface roughness *Sa* of almost 1 µm) that allows for mechanical interlocking as adhesion mechanism. The annealing treatment leads to the formation of an oxide layer rich in magnesium hydroxide $Mg(OH)_2$. This layer allows for chemical bonding together with a slight mechanical interlocking thanks to the irregular and porous nature of the oxide, characterized by reentrant surfaces. The combination of the two surface treatments allows for simultaneous chemical bonding and strong mechanical interlocking. The interface energy in opening mode (mode I) G_I is reported in Fig. 2 as well. The values show that the sole annealing leads to a more reliable joining than sandblasting, whilst their combination permits a substantial increase in the joining strength. It is worth to underline that the treatments carried out on the AZ31B sheets did not impacted on the mechanical properties of the material since the microhardness variations were within 2%.

Table 2. AZ31B sheets surface treatments before joining.

Surface treatment	Notes	Sample name
Sandblasting	4 bar pressure with F120 white corundum (1)	SB
Annealing	500°C for 20 minutes followed by air cooling (2)	A
Sandblasting + annealing	Sandblasting (1) followed by annealing (2)	SB+A

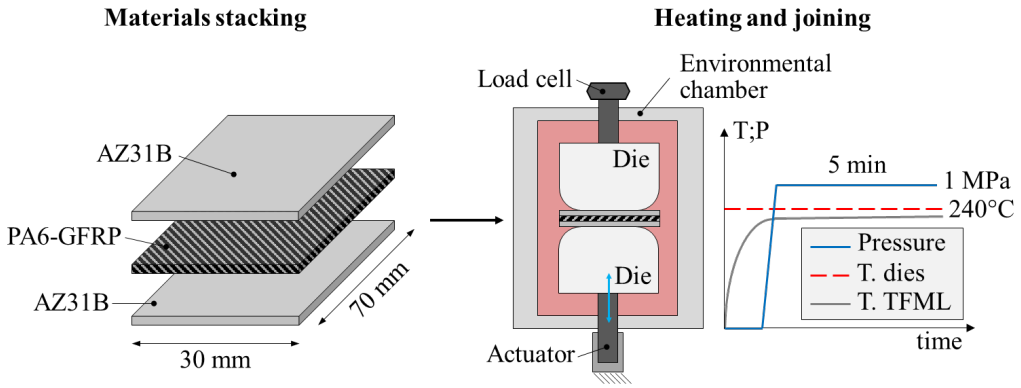

Fig. 1. Material stacking and geometry of the TFML (left) and HMP process for fabricating the TFML (right).

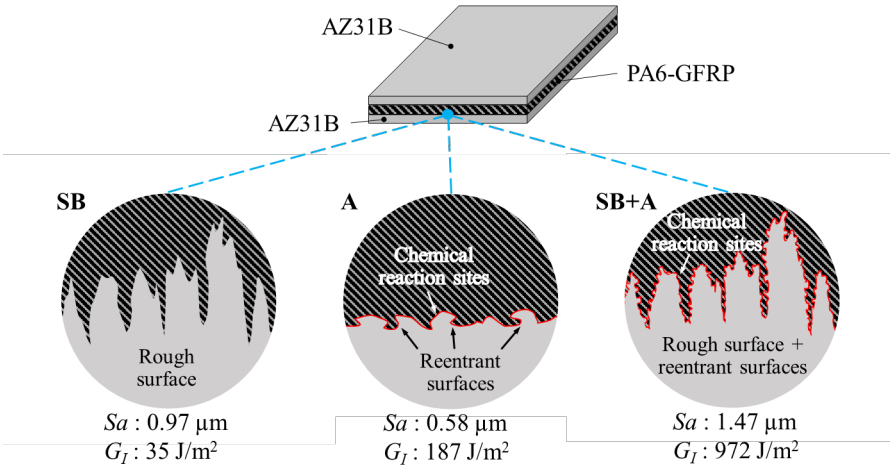

Fig. 2. Representation of the different interfaces after HMP at varying AZ31B surface treatment.

TFMLs drilling trials. The drilling trials were conducted on a high-precision machining center Micromaster™ 5X by Kugler. The machine is equipped with an aerostatic spindle speed up to 60˙000 rpm and a vertical axis run-out lower than 2 µm. The experimental setup is shown in Fig. 3. It

consisted of a setup for fixturing the TFML, a 3-component piezoelectric dynamometer (type 9119AA2 from Kistler™) connected to a charge amplifier (LabAmp 5167A from Kistler™), and a personal computer for data acquisition and elaboration via the DynoWare™ software. The dynamometer was mounted on the CNC machining table. The TFMLs workpieces were clamped in a stiff steel back-up fixture with 5 mm thickness fixed on the dynamometer table thorough four screws at the TFMLs extremities.
The tools used for the experiments were 3 mm diameter uncoated solid carbide drill bits with twist and spur geometries, as reported in Fig. 4. The twist drill bit is characterized by a 118° point angle and a 25° helix angle. The spur drill bit presents a point design that is optimized for composite drilling, and a helix angle of 25°. The integrity of each drill bit utilized for the drilling trials was checked using a FEI™ QUANTA 450 Scanning Electron Microscope (SEM) prior to machining. Drilling operations were carried out in dry conditions, which is usually preferred when machining aeronautical components to avoid the need of cleaning prior to assembly and obtain high-quality holes at reduced time and costs [13]. Two levels of feed *f* were considered keeping constant the cutting speed, namely 0.07 mm/rev and 0.30 mm/rev, at 40 m/min. The SB, A and SB+A TFMLs were drilled with 6 mm spaced through holes. The thrust force *Fz* of the drilling operations was measured with the dynamometer at a sampling rate of 10 kHz. Three trials were performed on each TFML type (SB, A, and SB+A) for each set of cutting parameters, for a total of 36 drilling operations. To prevent any effect of tool wear, or built-up edge formation, each TFML was drilled with a fresh drill bit. The experimental plan for the drilling operations is reported in Table 3.

Hole quality characterization. To evaluate the hole quality, the TFMLs were sectioned at the middle of the holes using an abrasive cut off saw for metallographic investigations. The internal surface of the holes was inspected using the SEM in low vacuum mode to observe both the conductive AZ31B and the non-conductive PA6-GFRP without coating the samples. The quality of the holes was evaluated in terms of surface finishing, adhered material, fibers pull out, PA6 matrix smearing, and delamination at the interfaces.

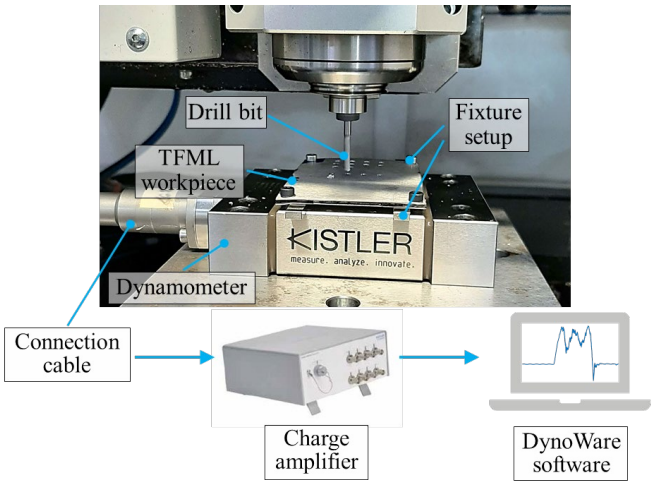

Fig. 3. Experimental setup for the drilling operations.

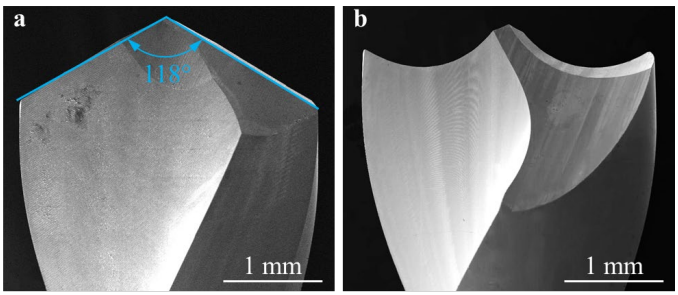

Fig. 4. SEM images of the 3 mm Ø drill bits: twist (a) and spur (b) geometries.

Table 3. Experimental plan for the drilling operations.

	Factors		
	Drill feed	Drill bit	TFML type
Level 1	0.07 mm/rev	twist	SB
Level 2	0.03 mm/rev	spur	A
Level 3	/	/	SB+A

Results and Discussion

Thrust forces. Fig. 5 reports typical thrust force diagrams when drilling A and SB+A TFMLs. The curves present a general trend in which are distinguishable the response of the AZ31B sheets at the extremities and the one of the PA6-GFRP core. The thrust force diagram shows also two valleys that are representative of the response of the interfaces as illustrated in the first diagram on the left of Fig. 5. The drill feed has the main effect on the thrust force: at increasing feed, the forces increase by 123% since the higher the strain rate the higher the material strength, therefore the recorded force. On the contrary, the thrust force reduction using the spur drill bit rather than the twist one is not significant (-5% on average). However, the spur geometry allowed for a reduction in the elastic inflection of the TFML under the drill point load when exiting the workpiece, which is known to be the main delamination cause in such workpieces [14]. This is suggested by the absence of disturbances in the force signal in the final part of the curve as the chisel edge exits the second AZ31B magnesium sheet (indicated in the diagrams by the blue arrows). The most relevant difference between the two drill bits is noticeable when observing the thrust force diagrams obtained when drilling with the higher feed, i.e. 0.30 mm/rev. The twist drill bits weren't able to perform a through hole and the drill stopped in the magnesium sheet before reaching the end of the stroke due to the excessive tensile forces perceived by the spindle activating the rotation lock system of the CNC machine. The thrust force diagrams show, in fact, a wide negative (tensile force in the direction of the spindle axis) thrust force peak at the chisel edge exit from the workpiece. On the contrary, the spur drill bit was able to perform the through holes with just a little workpiece inflection under the drill bit. The TFML type had a little effect on the thrust force mean values, nevertheless it had an impact on the recorded forces at the interface.

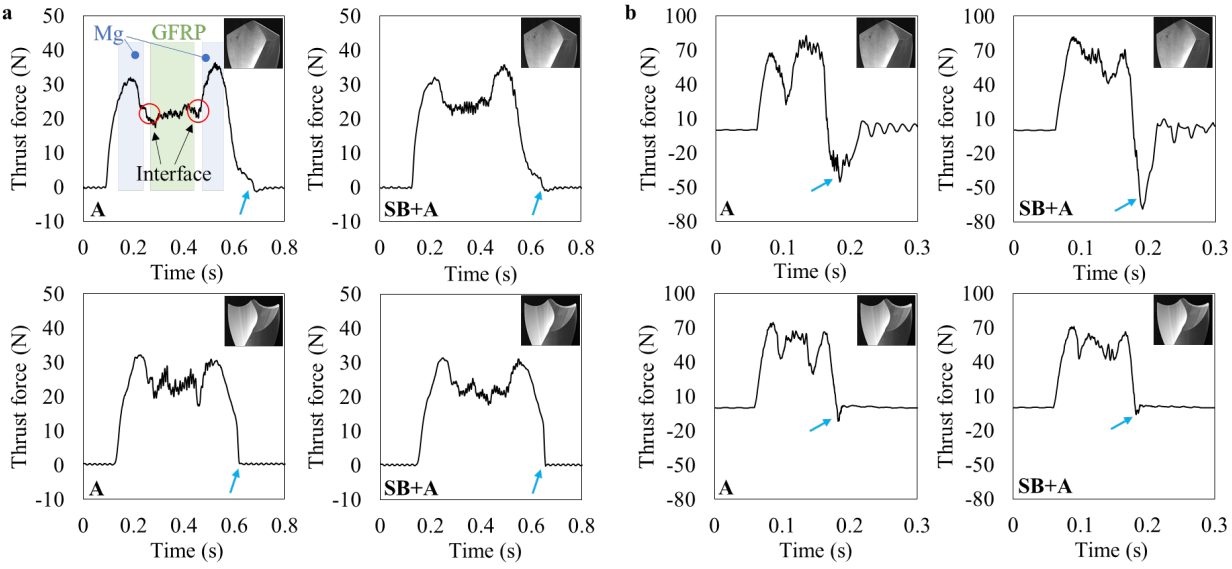

Fig. 5. Thrust force diagrams when drilling A and SB+A TFMLs at varying drill bit geometry and drill feed, namely at 0.07 mm/rev (a) and 0.30 mm/rev (b).

Fig. 6 report the mean thrust forces at the two interfaces between the metal sheet and the GFRP at varying of the investigated parameters. It is possible to observe that the forces at the interface were

higher for the SB+A TFML. In particular, the latter presented + 28% and + 45% higher forces than the SB and A TFML, respectively. This can be related to the interface resistance to delamination in drilling. In fact, it is known that delamination usually occurs due to push-down forces [15], especially intense at the drill exit. The results of Fig. 6 suggest that the SB+A TFML interface is more resistant than the one of the SB TFML, which, in turn, is more resistant than the A TFML interface. This was especially verified at the higher drill feed. The drilling forces output can be related to the surface energy in mode I of the different surface treatments as reported in Fig. 2. The calculated surface energy of the SB+A interface was largely greater than the ones of the other two cases, being the energy of the SB interface the lowest. Nevertheless, when drilling, the behavior of the SB and A interfaces reversed: this means that, under the drilling forces and phenomena that may occur during cutting, such as temperature increase, the chemical bonding becomes less effective than the mechanical interlocking. Although, the combined effect of chemical and mechanical bonding (SB+A case) is confirmed.

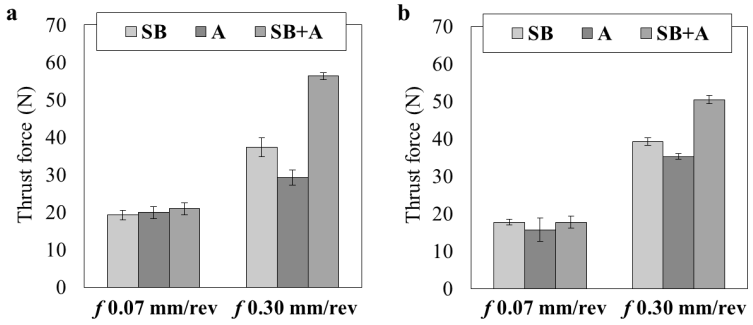

Fig. 6. Mean thrust forces at the interface as a function of the TFMLs type and drill feed when drilling with twist (a) and spur (b) drill bits.

Holes quality. Fig. 7 reports the holes cross sections of the SB+A TFML at varying drill bit geometry and drill feed. The higher drill feed led to a lower quality of the hole internal surfaces, with visible feed marks and adhered material on the magnesium sheets hole surfaces. Whereas, the PA6-GFRP surfaces presented higher amount of fiber pull out and matrix smearing at the higher feed. The interfaces presented smeared PA6 as well. The observed features can be related to the higher thrust forces developed when using the higher drill feed, which led to higher cutting temperatures that may be considered responsible of the aforementioned defects.

The effect of the different drill bits geometry on the hole quality is visible mainly at the higher feed. As commented for the thrust force diagrams, the twist geometry was not able to obtain a through hole, as visible in the images at the lower left part of Fig. 7, whilst the spur bit allowed for a good quality hole.

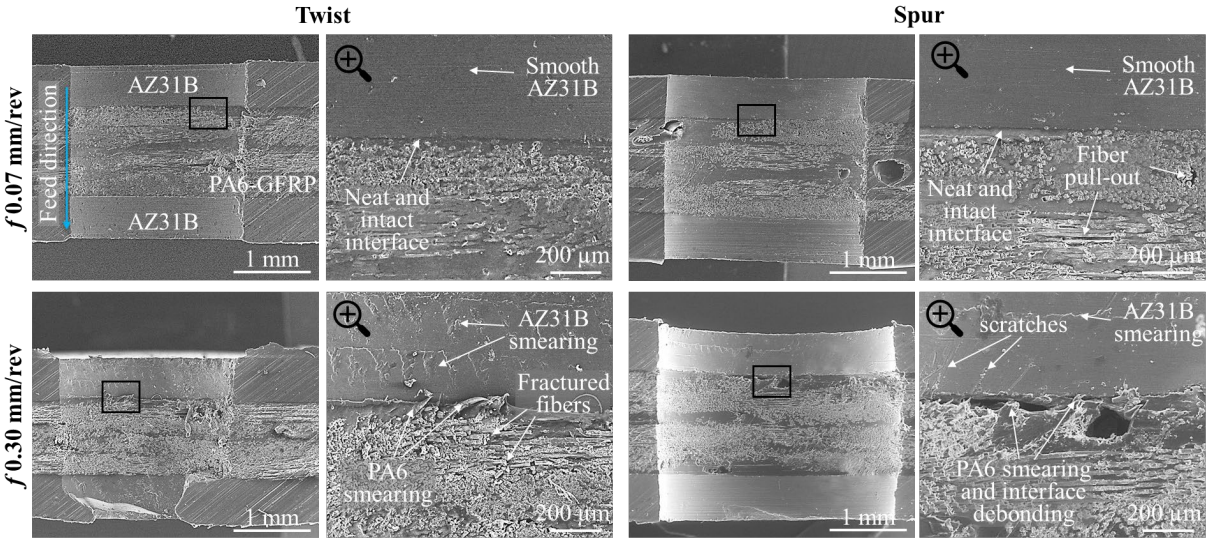

Fig. 7. Hole sections of the SB+A TFMLs at varying drill bit geometry and drill feed.

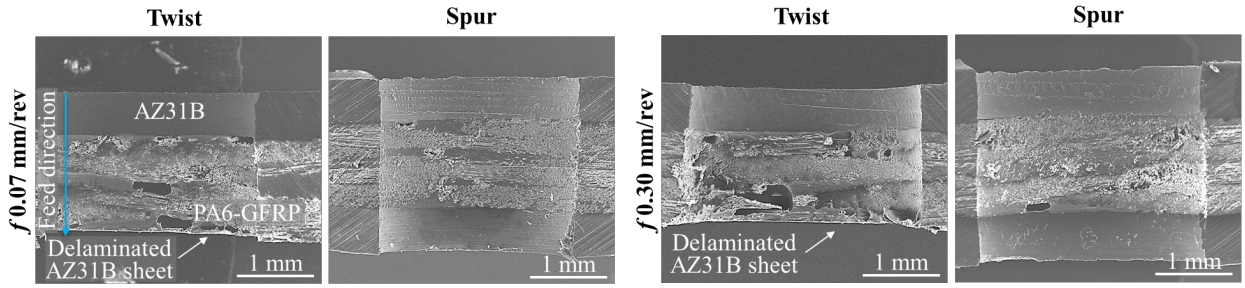

Fig. 8. Holes sections of the SB TFMLs at varying drill bit geometry and drill feed.

It is worth underlining that the SB+A TFML was the only one that did not present delamination regardless of the other parameters (see Fig. 7), in agreement with the thrust force results. In the case of the A TFML the delamination at the exit interface indeed occurred in the great majority of the cases, whilst in the case of the SB TFML the drill bit geometry played a role in determining the delamination. Fig. 8 shows the SB TFML hole sections at varying drill bit geometry and drill feed: it is possible to observe that the twist drill bit led to delamination (the second magnesium AZ31B sheet is missing), whilst the spur drill bit prevented the magnesium sheet detachment.

Conclusions

In this work, the drillability of FMLs joined via HMP was investigated at two levels of feed and drill bit geometry, namely uncoated twist and spur drills. The FMLs were composed of a thermoplastic GFRP core and AZ31B magnesium alloy external sheets previously treated through sandblasting, annealing, and their combination to increase the joining strength. The thrust force, hole quality, delamination and fiber pull-out were considered to evaluate the FMLs drillability. The following conclusions can be drawn:

- The greater drill feed resulted in a 123% increase in thrust force over the lower drill feed.
- Spur drill bits improved the drillability avoiding delamination and increasing the hole quality (reduced polymer matrix and AZ31B smearing), especially at the higher drill feed. The better drillability with the spur geometry can be ascribed to the reduced FML inflection under the drill bit load.
- Sandblasting in combination with annealing of the AZ31B sheets allowed the highest drillability, avoiding delamination thanks to the higher interfaces bonding.
- The sole annealing of the AZ31B sheets led to the highest incidence of delamination, despite the surface energy of the bonding of these sheets is higher than the one of the sandblasted sheets. This can be ascribed to the chemical bonding failure under the temperature increase during dry drilling.

References

[1] Kavitha K, Vijayan R, Sathishkumar T. Fibre-metal laminates: A review of reinforcement and formability characteristics. Mater. Today Proc. 22 (2020) 601–5.

[2] Sarasini F, Tirillò J, Ferrante L, Sergi C, Sbardella F, Russo P, et al. Effect of temperature and fiber type on impact behavior of thermoplastic fiber metal laminates. Compos. Struct. 223 (2019) 110961.

[3] Ding Z, Wang H, Luo J, Li N. A review on forming technologies of fibre metal laminates. Int. J. Light Mater. Manuf. 4 (2021) 110–26.

[4] Bruschi S, Cao J, Merklein M, Yanagimoto J. Forming of metal-based composite parts. CIRP Ann. 70 (2021) 567–88.

[5] Cortés P, Cantwell WJ. The fracture properties of a fibre-metal laminate based on magnesium alloy. Compos. Part B Eng. 37 (2005) 163–70.

[6] Pärnänen T, Alderliesten R, Rans C, Brander T, Saarela O. Applicability of AZ31B-H24 magnesium in Fibre Metal Laminates - An experimental impact research. Compos. Part A Appl. Sci. Manuf. 43 (2012) 1578–86.

[7] Baldan A. Adhesively-bonded joints and repairs in metallic alloys, polymers and composite materials: Adhesives, adhesion theories and surface pretreatment. J. Mater. Sci. 39 (2004) 1–49.

[8] Arkhurst BM, Kim JH, Lee MY. Hot metal pressing joining of carbon fiber reinforced plastic to AZ31 Mg alloy and the effect of the oxide surface layer on joint strength. Appl. Surf. Sci. 477 (2019) 241–56.

[9] Ghiotti A, Bruschi S, Kain M, Lizzul L, Simonetto E, Tosello G. Simultaneous bonding and forming of Mg fibre metal laminates at high temperature. J. Manuf. Process 72 (2021) 105–14.

[10] Bertolini R, Savio E, Ghiotti A, Bruschi S. The effect of cryogenic cooling and drill dbt on the hole quality when drilling magnesium-based fiber metal laminates. Procedia Manuf. 53 (2021) 118–27.

[11] Bonhin EP, David-Müzel S, de Sampaio Alves MC, Botelho EC, Ribeiro MV. A review of mechanical drilling on fiber metal laminates. J. Compos. Mater. 55 (2021) 843–69.

[12] ASTM E92: Standard Test Methods for Vickers Hardness and Knoop Hardness of Metallic Materials 2017.

[13] Aamir M, Giasin K, Tolouei-rad M, Vafadar A. A review: drilling performance and hole quality of aluminium alloys for aerospace applications. J. Mater. Res. Technol. 9 (2020) 12484–500.

[14] Capello E. Workpiece damping and its effect on delamination damage in drilling thin composite laminates. J. Mater. Process Technol. 148 (2004) 186–95.

[15] Park SY, Choi WJ, Choi CH, Choi HS. Effect of drilling parameters on hole quality and delamination of hybrid GLARE laminate. Compos. Struct. 185 (2018) 684–98.